Supplementary Information (SI) for Materials Horizons.
This journal is © The Royal Society of Chemistry 2025

Supplementary Information

Method for measuring exciton-exciton annihilation rate constants in thermally activated delayed fluorescent emitters to understand efficiency roll-off in OLEDs

Le Zhang,[a b +] Arvydas Ruseckas,* [a +] Kou Yoshida,[a] Liam G. King,[a] Subeesh Madayanad Suresh,[b] Eli Zysman-Colman,* [b] and Ifor D.W. Samuel* [a]

[a] Organic Semiconductor Centre, SUPA, School of Physics and Astronomy, University of St. Andrews, St. Andrews, KY16 9SS, U.K. E-mail: ar30@st-andrews.ac.uk and idws@st-andrews.ac.uk

[b] Organic Semiconductor Centre, EaStCHEM School of Chemistry, University of St Andrews, St Andrews, KY16 9ST, UK. E-mail: Email: eli.zysman-colman@st-andrews.ac.uk

[+] These authors contributed equally to this work

1. Prompt and delayed fluorescence at low excitation density and rate constants

The PL decays of **DABNA-2** were measured using the incident excitation fluence of 0.5 μJ/cm^2 at 375 nm. The decay time of the prompt fluorescence (PF) is τ_{PF}=5.4 ns, whilst that of delayed fluorescence (DF) τ_{DF}≈100 μs, both showing no significant variation as a function of DABNA-2 concentration.

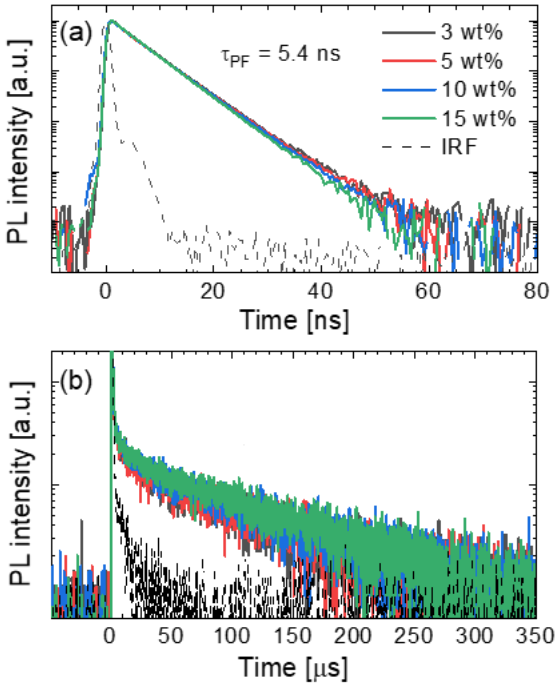

Figure S1. Kinetics of prompt fluorescence (a) and delayed fluorescence (b) of **DABNA-2** in mCBP films at different concentrations measured at 468 nm using time-correlated single photon counting and multi-channel scaling techniques, respectively. The instrument response functions (IRF) are shown as dashed lines. Excitation wavelength was 375 nm.

The PF and DF contributions to the PLQY were estimated by taking the area under the corresponding PL decay curves, which give Φ_{PF}= 0.75 and Φ_{DF} = 0.07. The other rate constants were found using[1]

$k_S = \Phi_{PF}/\tau_{PF}$=1.39 × 10^8 s^{-1};

$\Phi_{PF} = k_S/(k_S + k_{ISC})$, k_{ISC} = 1.6 × 10^7 s^{-1};

$k_{RISC} = \frac{k_{PF}k_{DF}}{k_{ISC}}\frac{\Phi_{DF}}{\Phi_{PF}}$ =1.1×10^4 s^{-1}

2. Distribution of DABNA-2 molecules in mCBP host

In order to test the distribution of **DABNA-2** molecules in blend films we excited the mCBP host at 343 nm and measured the kinetics of electronic energy transfer (EET) from mCBP to **DABNA-2** by time-resolved PL using the streak camera in synchroscan mode (Figure **S2ab**). Nearly mono exponential decays of mCBP emission and the corresponding rise of **DABNA-2** emission are observed which indicate that EET occurs with well-defined rate constants and points to a diffusion-mediated EET to **DABNA-2** molecules which are homogeneously dispersed in mCBP matrix. The EET rate constant is approximately proportional to the density of **DABNA-2** molecules at least up to 10 wt% which indicates no significant aggregation of **DABNA-2** molecules up to 10 wt% (Figure **S2c**).

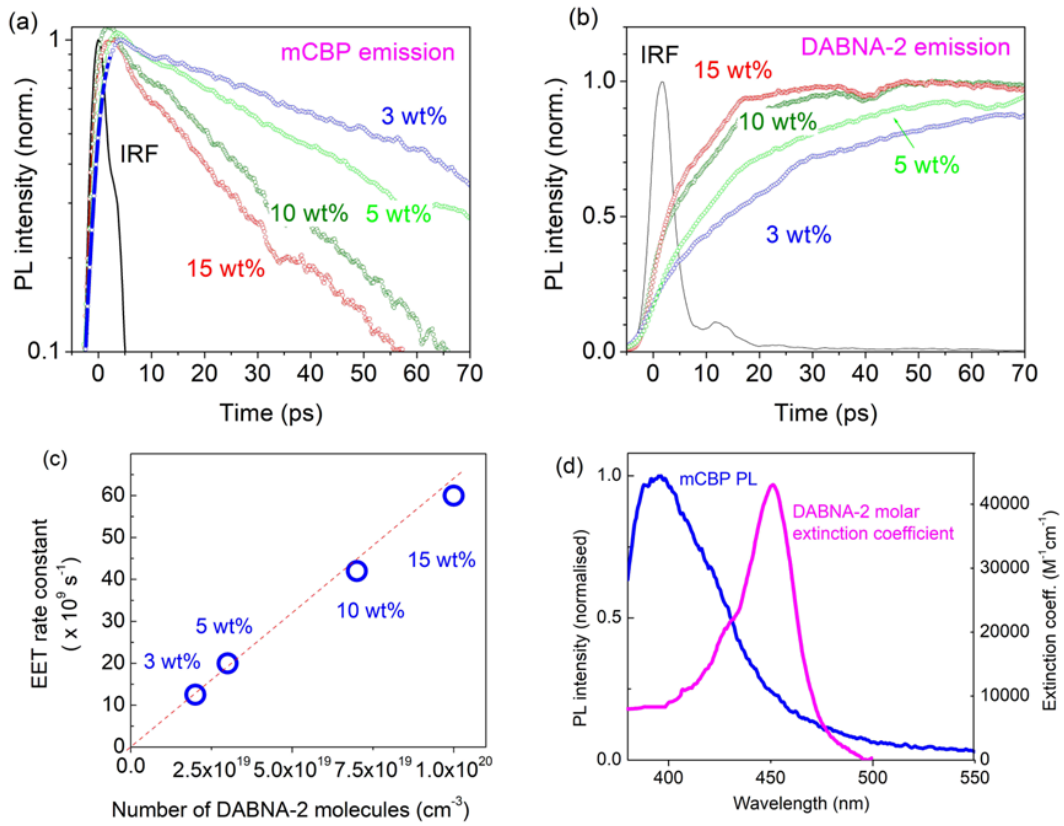

Figure S2. Time-resolved PL intensity of mCBP (a, detection 350-400 nm) and **DABNA-2** (b, detection 450-500 nm) in blend films with different concentrations of **DABNA-2** in mCBP host following excitation at 343 nm. IRF is the instrument response function. (c) The rate constant of energy transfer from mCBP to **DABNA-2** vs the density of DABNA-2 molecules, the dotted line indicates the proportionality. (d) Spectral overlap of mCBP PL and DABNA-2 absorption.

The rate constant of the diffusion-mediated EET k_{EET} can expressed by the Smoluchowski equation

$$k_{EET} = 4\pi D_s N_a R_c \qquad \text{(S1)}$$

where D_s is the singlet exciton diffusion coefficient in mCBP, N_a is the density of **DABNA-2** molecules and R_c is the capture radius of mCBP exciton by **DABNA-2** molecules. The exciton capture occurs by non-radiative Förster resonance energy transfer (FRET) from mCBP to **DABNA-2** because mCBP PL spectrum overlaps with **DABNA-2** absorption (Figure **S2d**). It has been shown that

$$R_c \approx 0.676 \left(\frac{R_0^6}{\tau D_s}\right)^{1/4} \qquad \text{(S2)}$$

In this case R_0 is the Förster radius for FRET from mCBP to DABNA-2 and τ=1ns is the singlet exciton lifetime in mCBP. Using the Förster equation and the overlap of the measured spectra in Fig. S2d we calculate R_0 = 1.4 nm. Then from Equations S1 and S2 we obtain D_s = 0.002 cm^2s^{-1} in mCBP which is similar to D_s = 0.003 cm^2s^{-1} measured in films of CBP.[2] Slightly lower D_s for mCBP as compared to CBP is not surprising because mCBP films are more disordered than CBP. By taking the ratio of k_{EET} to $k_{EET}+\tau^{-1}$, we determined the energy transfer efficiency to be 93% and 95% for films with 3 and 5 wt% of **DABNA-2**, respectively, whilst for films with 10 and 15 wt% **DABNA-2** it is ~98%.

3. The effect of singlet-singlet annihilation (SSA)

To determine the effect of SSA on the exciton population we measured PL decays using a range of pulse densities. The PL decays measured at a pulse density of 5 μJ/cm^2 and 10 μJ/cm^2 are nearly identical which shows that SSA has no significant influence at this density (Figure S3).

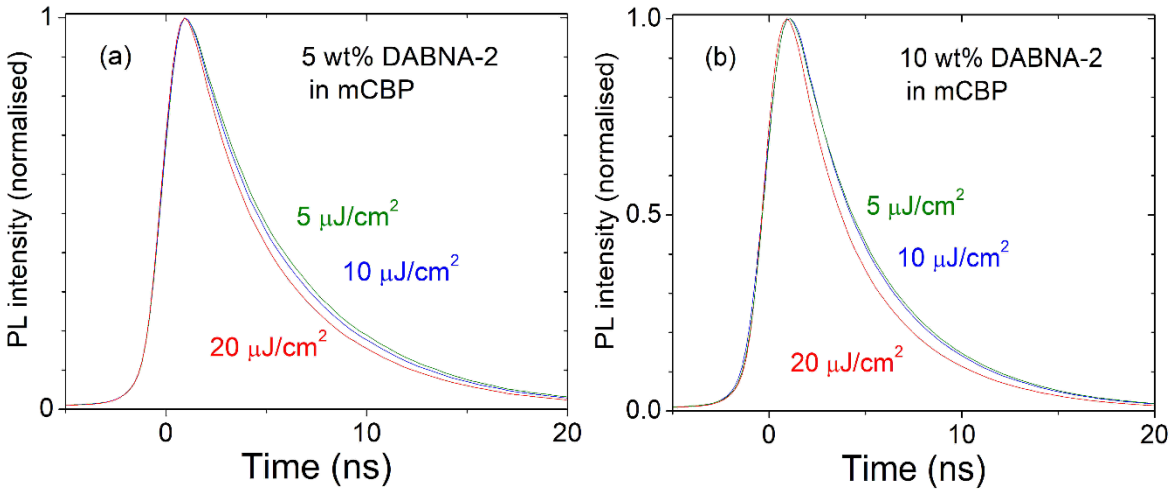

Figure S3. Photoluminescence kinetics in the 5 wt% DABNA-2:mCBP film (a) and 10 wt% (b) measured at 2 kHz with different pulse energy densities.

4. Quenching dynamics for different pulse densities

Taking the ratio of the time-resolved fluorescence intensities measured at the high and low f_{rep} , i.e., $PL\ ratio = {I(high\ f_{rep})}/{I(2\ kHz)}$ divides out other decay channels of singlet excitons and gives a direct measurement of the STA effect. We find that quenching by triplets at t>10 ns can be well approximated to a mono-exponential decay as shown by the linear fits to the natural logarithm of the PL ratio in Figure S4. This indicates that the quenching rate is defined by the singlet exciton diffusion to the quencher on this time scale. The faster quenching component at t<10 ns is more pronounced when using a higher pulse density of 10 μJ/cm^2 and a higher f_{rep} , and is attributed to the direct Förster resonance energy transfer (FRET) to triplets which are within the Förster radius from photogenerated singlets.

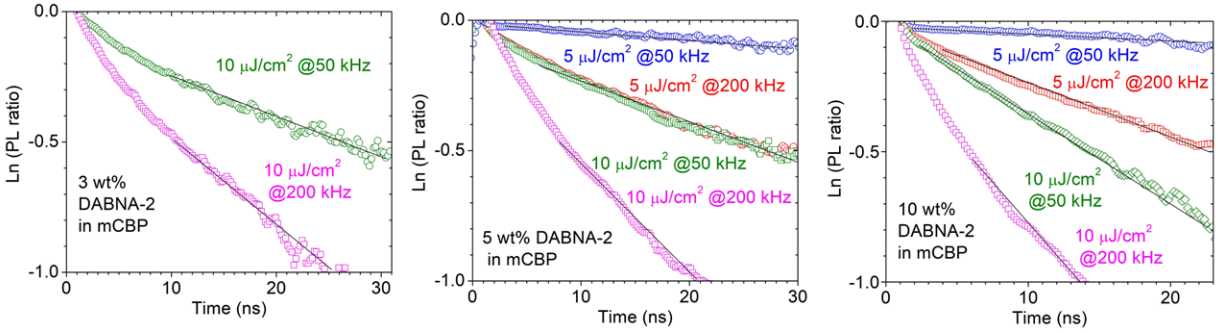

Figure S4. Natural logarithm of the PL ratio (symbols) measured with varying f_{rep} of excitation pulses and the incident pulse density. Solid lines are fits to Equation 3.

5. Determining the steady-state triplet density and γ_{TTA}

The density of singlet excitons in **DABNA-2** generated by a single excitation pulse, N_0 , was determined using

$$N_0 = \frac{f\,W\,Q}{L\,E_{phot}} \qquad \text{(S3)}$$

where f=0.35 is the fraction of light absorbed in the film determined by subtracting the transmitted and reflected light intensities, W is the incident pulse density in J/cm^2, Q is the energy transfer efficiency to **DABNA-2**, L=50 nm is the film thickness, and E_{phot} is the photon energy. The steady-state triplet exciton density, N_T, was calculated using Equations 1 and 2 in the main paper with G=N_0 f_{rep} and ${dN_S}/{dt} = {dN_T}/{dt} = 0$ whilst varying γ_{TTA} from 10^{-17} to 10^{-11} cm^3 s^{-1}. The calculated N_T at different laser repetition rates and the ratio r = N_T(200 kHz)/N_T(50 kHz) are shown in Figure **S5**. For γ_{TTA}< 10^{-15} cm^{3}s^{-1} the ratio r≈ 3.5 is close to the ratio of the singlet generation rate at 200 kHz and 50 kHz, the small difference being due to RISC and delayed fluorescence. As γ_{TTA} increases, the ratio, r, decreases sharply and reaches r = 2 at γ_{TTA} >10^{-13} cm^{3}s^{-1}. This is the classical multistep-diffusion-assisted TTA limit where the triplet exciton density at infinity follows the square root dependence on the exciton generation rate.

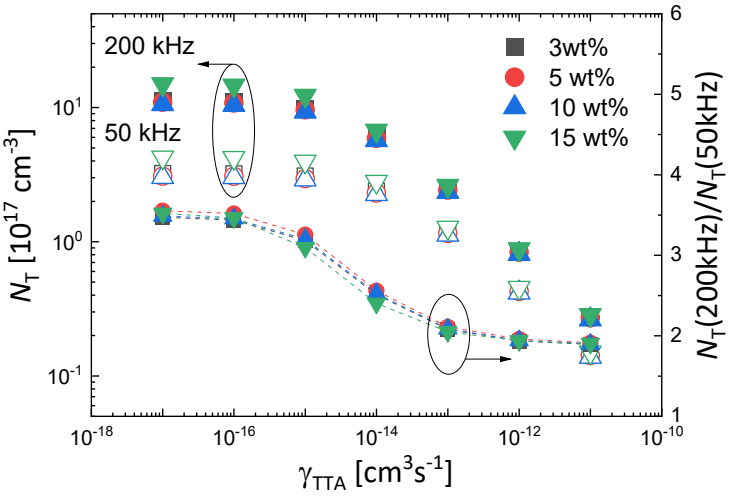

Figure S5. Steady-state triplet exciton density (N_T) calculated at different laser repetition rates using an incident pulse density of 10 μJ/cm^2 and their ratio as a function of the triplet-triplet annihilation (TTA) rate constant γ_{TTA}.

Because the effect of TTA on N_T is very weak for $\gamma_{TTA} < 10^{-15}$ cm^3 s^{-1} , we considered γ_{TTA} in the range 10^{-15} – 10^{-13} cm^3 s^{-1}. For each value of γ_{TTA} we calculated the triplet density and used this to determine different values of γ_{STA} as shown in Figure 4. We then measured the delayed fluorescence lifetime of DABNA-2 in the films under the background illumination by a continuous wave (CW) 450 nm laser diode to generate a large exciton population (Figure **S5**). Then we fitted the delayed PL lifetime with different γ_{TTA} to refine the γ_{TTA} value. This process resulted in a best-fit value of γ_{TTA} = 1.3 × 10^{-14} cm^3 s^{-1} for 10 wt% DABNA-2: mCBP. For 5 wt% there is a considerable spread of data. Considering Figure S6(b) and noting that for a fit to γ_{TTA} of 1×10^{-14} cm^3 s^{-1}, nearly all data points are above the fit, we take 10^{-14} cm^3 s^{-1} as an upper limit for considered γ_{TTA}. Additional lines are also included to show the effect of mis-fitting the data.

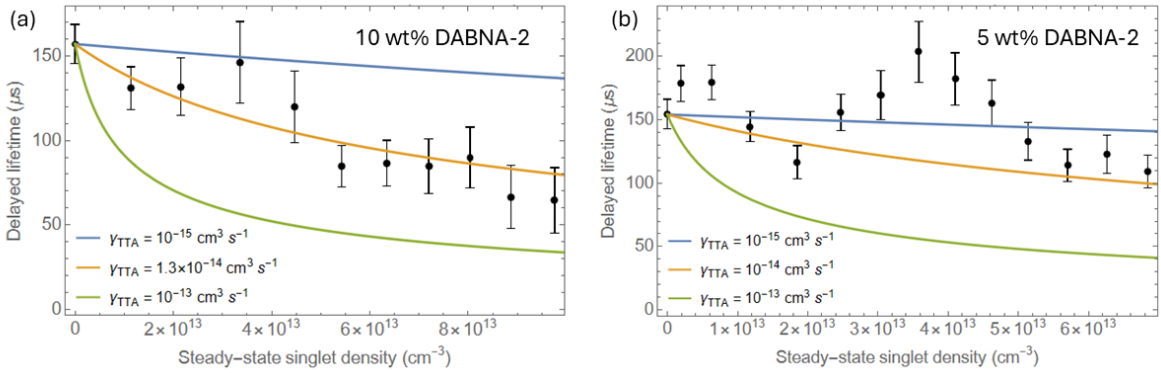

Figure S6. Delayed PL lifetime data for the 10 wt% DABNA-2: mCBP film (a) and 5 wt% (b) with fits shown for different γ_{TTA} values.

As a further check of the upper limit, we considered scaling of γ_{TTA} with intermolecular distance. Because TTA is mediated by triplet exciton diffusion which occurs by an electron exchange mechanism, the rate of triplet-triplet energy transfer (k_{TET}) decreases exponentially with the distance R between molecules $k_{TET} \propto \exp(-\beta R)$ where β is the attenuation factor. Typically β >1 Å^{-1} is observed in organic glasses as well as between chromophores

linked through nonconjugated bridges, but lower β values of 0.64 Å^{-1} and 0.39 Å^{-1} have been reported for chromophores linked through p-phenylene bridges.[3] We estimate the average distance between adjacent DABNA-2 molecules in the mCBP host to be $c_D^{-1/3}$. This gives 3.1 nm for 5 wt% DABNA-2 film and 2.5 nm for 10 wt%. Even with the lowest reported β=0.39 Å^{-1} we estimate the rate of triplet-triplet energy transfer for 5 wt% DABNA-2 to be ten times lower than for 10 wt%. Because γ_{TTA} is approximately proportional to k_{TET}, its value in 5 wt% DABNA-2 film is predicted to be at least ten times lower than in the 10 wt% film.

6. EQE roll-off simulation

Under electrical excitation, the singlet and triplet exciton densities, N_S and N_T, are described by

$$dN_S/dt = \frac{1}{4}\gamma_{eh}N_p{}^2 - \left(k_S + k_{ISC} + \gamma_{STA}N_T + \gamma_{SPQ}N_P\right)N_S + k_{RISC}N_T + 0.25\gamma_{TTA}N_T^2 \quad \text{(S5)}$$

$$dN_T/dt = \frac{3}{4}\gamma_{eh}N_p{}^2 + k_{ISC}N_S - k_{RISC}N_T - 1.25\gamma_{TTA}N_T^2 \quad \text{(S6)}$$

Here, N_p is the density of recombining charge pairs, γ_{eh} is the recombination rate constant, γ_{SPQ} represents singlet quenching by polarons, the other rate constants are defined in Equations 1 and 2 in the main paper. Here again we assumed that TTA in OLEDs generates singlet and triplet excitons with a 1:3 ratio. At the upper limit of γ_{TTA}< 10^{-14} cm^3 s^{-1} which we found in films with 5 wt% DABNA-2, the TTA contribution to the singlet population is very small, therefore, the ratio has no significant effect on the EQE roll-off. The singlet and triplet densities under the steady-state condition were calculated using $dN_S/dt = dN_T/dt = 0$ and assuming that all injected charges form excitons, hence

$$\gamma_{eh}N_p{}^2 = \frac{j}{ew} \quad \text{(S7)}$$

Here, j is the steady-state current density, e is the elementary charge, w is the width of the recombination zone. The EQE roll-off was simulated as the ratio of N_s values calculated with and without annihilation losses and normalised to the experimental EQE maximum. First, we simulated the EQE roll-off assuming w=20 nm which is the thickness of the light emitting layer and found that TTA reduces STA losses at high current very slightly (Figure **S7**). The predicted EQE roll-off by STA is not as severe as experimentally observed. This indicates that other exciton loss mechanism should be considered besides STA and/or the width of the recombination zone w<20 nm.

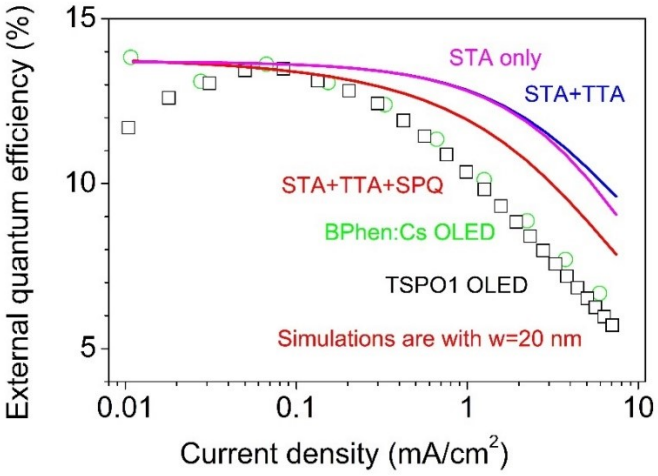

Figure S7. Experimental EQE of OLEDs with 5 wt% **DABNA-2** in mCBP host driven at constant current (symbols) and simulated EQE (lines) using the measured γ_{STA} = 6 × 10^{-11} cm^3 s^{-1} , γ_{TTA} = 1 × 10^{-15} cm^3 s^{-1} and γ_{SPQ} =γ_{STA}. The width of the recombination zone was set to *w*=20 nm which is the thickness of the light emitting layer.

Next, we considered the quenching of singlets by polarons (SPQ). The electron-hole recombination rate in OLEDs is limited by carrier diffusion in directions perpendicular to the electric field and is governed by the zero-field charge mobility.[4,5] Then, assuming Langevin-type recombination,

$$\gamma_{eh} = \frac{e(\mu_{0e}+\mu_{0h})}{\varepsilon_0 \varepsilon} \qquad \text{(S8)}$$

Here μ_{0e} and μ_{0h} is the zero-field electron and hole mobility, respectively, whilst ε_0 and ε are vacuum and relative permittivity. Combining Equations (S7) and (S8) we get

$$N_p = \frac{1}{e}\sqrt{\frac{j\varepsilon_0\varepsilon}{(\mu_{0e}+\mu_{0h})w}} \qquad \text{(S9)}$$

To estimate carrier mobilities in the recombination zone, we have fabricated single-carrier devices with different **DABNA-2** concentrations. In electron-only devices (EODs) we used electron transporting layers of 1,3,5-tri(*m*-pyrid-3-yl-phenyl)benzene) (TmPyPB), whilst in hole-only devices (HODs) the hole transporting layer of 1,1-bis[(di-4-tolylamino)phenyl]cyclohexane (TAPC) was used. The structures were as follows:

EOD: ITO/TmPyPB(20 nm)/x% **DABNA-2**:mCBP(50 nm)/TmPyPB(20 nm)/LiF(0.8 nm)/Al

HOD: ITO/TAPC(20 nm)/x% **DABNA-2**:mCBP(50 nm)/TAPC(20 nm)/Al

The current density in EODs and HODs decreased about three times with the introduction of **DABNA-2** into the mCBP host, indicating that the transport of electrons and holes is controlled by trapping-release on **DABNA-2** (Figure **S6**). This is consistent with the ionization energy of **DABNA-2**

(5.38 eV) being substantially lower than that of mCBP (6.07 eV) and electron affinity higher (2.75 and 2.55 eV for **DABNA-2** and mCBP, respectively).[6]

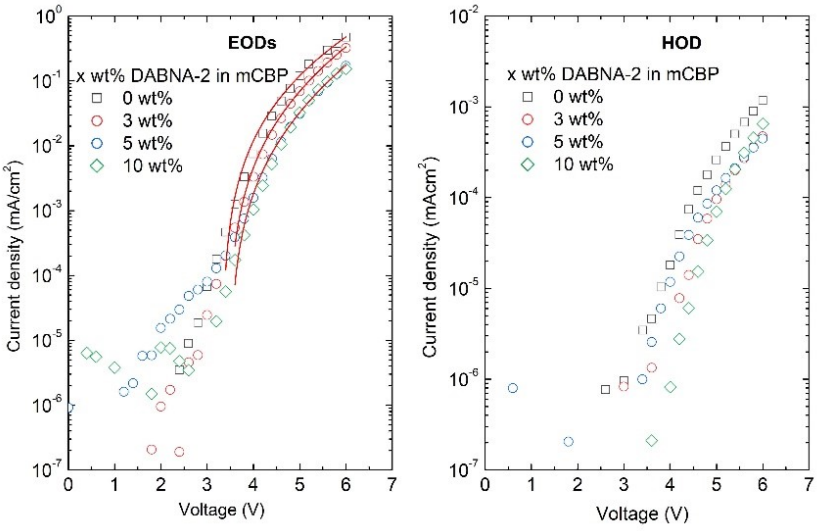

Figure S8. The J-V characteristics of single-carrier devices with different **DABNA-2** concentrations. The red lines for EODs represent the fits with Equation S10.

High electron mobility has been reported in TmPyPB, ~1×10^{-3} $cm^2 V^{-1}s^{-1}$ at 6.4×10^5 V cm^{-1} with a very weak dependence on the electric field.[7] There is just a small energy barrier for electron injection from TmPyPB into mCBP (electron affinities are 2.73 and 2.53 eV, respectively). At these conditions, the density of injected electrons is sufficiently high to form a space charge in the low conductivity mCBP layer. We fitted the current-voltage dependence in EODs with a space-charge limited current (SCLC) model according to the Mott-Gurney law.

$$J = \frac{9}{8}\varepsilon_0\varepsilon\,\mu_e\,\frac{(V-V_x)^2}{L^3} \qquad \text{(S10)}$$

Here V is the applied voltage, V_x is the onset voltage of SCLC regime, and L=90 nm is the thickness of the organic layer. This equation is only valid for $V>V_x$. We used a field-dependent mobility according to Poole-Frenkel mechanism.

$$\mu_e = \mu_{0e}\exp\left\{\beta_e\left[\frac{V}{L}\right]^{1/2}\right\} \qquad \text{(S11)}$$

Here, μ_{0e} is the zero-field electron mobility, and β_e is the Poole-Frenkel factor. The fitted parameters are given in Table S1. The μ_{0e} and β_e values for the EOD with a neat mCBP layer are similar to the previously reported $\mu_{0h}=7\times10^{-7}$ $cm^2 V^{-1} s^{-1}$, and β_h=0.017 values for holes,[8] suggesting that electron and hole mobilities in mCBP are reasonably well balanced. As we observed very similar decreases of the current density in EODs and HODs with the introduction of **DABNA-2** into a mCBP host, it is reasonable to assume $\mu_{0h}\approx\mu_{0e}$ for the mCBP layer with 5 wt % of **DABNA-2**. We use these mobilities

in Equation S5 to calculate the average density of charge pairs in the light-emitting layer. The predicted EQE roll-off by the combined effect of STA and SPQ for w=20 nm is still not as severe as experimentally observed (Figure **S7**). This suggests that the width of the recombination zone w<20 nm.

Table S1. Zero-field electron mobility μ_{0e} and the Poole-Frenkel factor β_{0e} obtained by fitting J-V dependence in EODs.

Emitter concentration in mCBP	V_x (V)	μ_{0e} (10^{-8} $cm^2 V^{-1} s^{-1}$)	β_e ($cm^{0.5} V^{-0.5}$)
0 wt% DABNA-2	3.32	90	0.006
3 wt% DABNA-2	3.44	14	0.008
5 wt% DABNA-2	3.48	3	0.009

References

1. K. Goushi, K. Yoshida, K. Sato and C. Adachi, *Nature Photonics*, 2012, **6**, 253-258.
2. A. Ruseckas, J. C. Ribierre, P. E. Shaw, S. V. Staton, P. L. Burn and I. D. W. Samuel, *Applied Physics Letters*, 2009, **95**, 183305.
3. V. Gray, B. Küçüköz, F. Edhborg, M. Abrahamsson, K. Moth-Poulsen and B. Albinsson, *Physical Chemistry Chemical Physics*, 2018, **20**, 7549-7558.
4. H. C. F. Martens, W. F. Pasveer, H. B. Brom, J. N. Huiberts and P. W. M. Blom, *Physical Review B*, 2001, **63**, 125328.
5. J. J. M. van der Holst, F. W. A. van Oost, R. Coehoorn and P. A. Bobbert, *Physical Review B*, 2009, **80**, 235202.
6. T. Hatakeyama, K. Shiren, K. Nakajima, S. Nomura, S. Nakatsuka, K. Kinoshita, J. Ni, Y. Ono and T. Ikuta, *Advanced Materials*, 2016, **28**, 2777-2781.
7. S. J. Su, T. Chiba, T. Takeda and J. Kido, *Advanced Materials*, 2008, **20**, 2125-2130.
8. A. S. D. Sandanayaka, K. Yoshida, T. Matsushima and C. Adachi, *The Journal of Physical Chemistry C*, 2015, **119**, 7631-7636.